Journal of Functional Foods 37 (2017) 330–338

Contents lists available at ScienceDirect

Journal of Functional Foods

journal homepage: www.elsevier.com/locate/jff

# *Phyllanthus emblica* L. (Indian gooseberry) extracts protect against retinal degeneration in a mouse model of amyloid beta-induced Alzheimer's disease

Holim Jang [a,b,1], Phisamai Srichayet [c,1], Woo Jung Park [d], Ho Jin Heo [e], Dae-Ok Kim [f], Sasitorn Tongchitpakdee [c], Tae-Jin Kim [g], Sang Hoon Jung [b,*], Chang Yong Lee [a,*]

[a] Department of Food Science, Cornell University, Ithaca 14850, USA
[b] Natural Products Research Center, Korea Institute of Science and Technology (KIST), Gangneung 25451, Republic of Korea
[c] Department of Food Science and Technology, Kasetsart University, Bangkok, Thailand
[d] Department of Marine Food Science and Technology, Gangneung-Wonju National University, Gangneung, Gangwon 26403, Republic of Korea
[e] Division of Applied Life Science, Institute of Agriculture and Life Science, Gyeongsang National University, Jinju 52828, Republic of Korea
[f] Department of Food Science and Biotechnology and Skin Biotechnology Center, Kyung Hee University, Yongin 17104, Republic of Korea
[g] Department of Biological Sciences, Pusan National University, Busan 46241, Republic of Korea

ARTICLE INFO

*Article history:*
Received 16 February 2017
Received in revised form 25 July 2017
Accepted 25 July 2017
Available online 20 September 2017

*Keywords:*
Indian gooseberry
Retinal degeneration
Alzheimer's disease
Amyloid beta

ABSTRACT

This study was to evaluate the protective effect of *Phyllanthus emblica* L. (Indian gooseberry) on retinal degeneration in a well-characterized animal model of Alzheimer's disease. RGC-5 cells were treated with Indian gooseberry extract (IGE), and intracellular antioxidant activity was evaluated. IGE was orally administered to mice for 21 days, then amyloid beta (Aβ) was administered by intracerebroventricular injection to induce neuronal damage in the brain and retina, and enucleated eyes were collected from the mice and analyzed using western blots and histological assays. As a result, we found that IGE inhibited intracellular oxidative stress and reduced the severity of histological changes caused by Aβ-induced retinal degeneration in retinal tissue. Furthermore, it regulated the levels of neurofilament (NF)-L, thymocyte differentiation antigen 1 (Thy-1), and sirtuin 1 (SIRT1) in the retina. These findings demonstrate that IGE protects against retinal degeneration and suggest that this effect is attributable to its antioxidant properties.



## 1. Introduction

Alzheimer's disease (AD) is an age-dependent neurodegenerative disorder that results in progressive loss of cognitive function (Wyss-Coray, 2006). Visual disturbances are a common symptom of AD (Mendez, Mendez, Martin, Smyth, & Whitehouse, 1990). Visual disturbances in AD patients consist of impairment in spatial contrast sensitivity, motion perception, and color discrimination, as well as blurred vision (Rizzo, Anderson, Dawson, Myers, & Ball, 2000; Rizzo, Anderson, Dawson, & Nawrot, 2000). Recent studies have demonstrated that visual impairment in AD patients may arise from retinal abnormalities, in addition to damage to the primary visual cortex and degeneration of cortical areas (Berisha, Feke, Trempe, McMeel, & Schepens, 2007; Guo, Duggan, & Cordeiro, 2010a). Several studies have demonstrated the formation of cataracts, loss of retinal neurons, retinal neuronal filament layer thinning, and impaired axonal outgrowth in AD patients (Chiu et al., 2012; Curcio & Drucker, 1993; Sadun & Bassi, 1990).

Although recent histological studies using optical coherence tomography and scanning laser polarimetry have shown retinal damage in AD patients, controversy remains because little is known of the mechanisms underlying this effect (Lu et al., 2010). One of the proposed mechanisms of retinal damage in AD is the accumulation of amyloid-beta (Aβ) peptide, which plays a prominent role in the pathology of AD. Aβ aggregates to form oligomers, protofibrils, and fibrils, which are deposited as amyloid plaque. Several lines of evidence indicate that amyloid plaque is involved in neuronal dysfunction and neurodegeneration, which is accompanied by increased levels of reactive oxygen species (Roher et al., 1993). Furthermore, Aβ deposits have been reported in glaucomatous optic nerve heads, drusen associated with age-related macular degeneration, and cataractous lenses (Dutescu et al., 2009). However, there are limited data demonstrating Aβ accumulation in the retinas of human AD patients.

* Corresponding authors.
*E-mail addresses:* shjung@kist.re.kr (S.H. Jung), cyl1@cornell.edu (C.Y. Lee).
[1] Holim Jang and Phisamai Srichayet contributed equally to this work.

http://dx.doi.org/10.1016/j.jff.2017.07.056
1756-4646/

*Phyllanthus emblica* L., commonly known as Indian gooseberry, is widely distributed in China, India, Indonesia, Malaysia, and Thailand, and its fruit has been used in many traditional medicines for atherosclerosis, diabetes, upset stomach, diarrhea, and skin problems (Barthakur & Arnold, 1991). Due to its high levels of vitamin C (412–900 mg/100 g) and minerals, Indian gooseberry fruit is used in juices, jams, and cosmetics (Jain & Khurdiya, 2004). Phytochemical investigations have reported that Indian gooseberry fruit extract contains tannins and various phenolic compounds, including ellagic acid, gallic acids and corilagin (Poltanov et al., 2009). In addition, Indian gooseberry has been shown to have antimicrobial, adaptogenic, antiatherogenic, antitussive, hepatoprotective, immunomodulatory, and chemoprotective activities (Liu, Zhao, Wang, Yang, & Jiang, 2008; Mayachiew & Devahastin, 2008b).

Interestingly, Indian gooseberry is used as a tonic and collyrium for eye disorders, and such use improves sight, reduces cataracts, and minimizes infections (Kumar et al., 2012; Srivasuki, 2012). A recent report showed that beta-glucogallin, a compound isolated from Indian gooseberry, had inhibitory effects on inflammatory eye-diseases such as uveitis by inhibiting aldose reductase (Chang et al., 2013). Other berries, such as blueberries, blackberries, and goji berries, have been considered beneficial to eye health because their constituent flavonoids, including anthocyanins, interact directly with rhodopsin and protect the retina from oxidative stress (Kalt, Hanneken, Milbury, & Tremblay, 2010). Indeed, oxidative stress plays a critical role in many age-related retinal diseases including age-related macular degeneration (AMD), and glaucoma (Wang, Kim, & Sparrow, 2017; Wang, Zhang, et al., 2015; Wang, Zhao, et al., 2015; Wang et al., 2016). Berry fruits also have neuroprotective effects on the brain, and have been shown to enhance neuroplasticity, neurotransmission, and calcium buffering (Miller & Shukitt-Hale, 2012). However, there is a lack of experimental studies regarding the efficacy of the retinal protective effect of Indian gooseberry.

Therefore, we hypothesized that oral administration of Indian gooseberry extract (IGE) would attenuate retinal degeneration caused by intracerebroventricular (ICV) injection of Aβ in an Alzheimer's disease mouse model. This is the first report of the protective effect of a berry fruit on retinal degeneration caused by direct injection of Aβ into the brain.

## 2. Materials and methods

### 2.1. Preparation of Indian gooseberry extract

Indian gooseberry fruits (cv. P-7) were obtained from experimental fields of Sithiporn Kridakorn Experiment Station, Agro-Ecological System Research and Development Institute, Kasertsart University, Prachuap Kiri Khan Province, Thailand. The fruits were collected in December 2012. The average fruit size was 2.32 ± 0.01 cm in diameter. The average fruit weight was 9.50 ± 0.37 g. The edible portion was approximately 89% of total fruit weight.

Ripe Indian gooseberry fruit from Thailand (brix 10.0–12.0, pH 2.3–2.5, and total acidity 2.1–2.8%) was freeze-dried and ground. The extract of Indian gooseberry fruit contained seed but its skin were removed. Ten grams of the freeze dried powder was mixed with 100 mL of deionized distilled water (DDW), and the resulting mixture was homogenized at 15,000 rpm for 2 min using a Polytron homogenizer (PT 10/35, Kinematica, Kriens-Luzern, Switzerland), filtered through Whatman #2 filter paper (Whatman International Ltd., Kent, U.K.), and rinsed with 50 mL of DDW. The homogenization procedure was repeated twice and the total volume of the mixture was adjusted to 500 mL. Liquid-liquid extraction was applied to the final mixture with equal volumes of the four organic solvents in the sequence of *n*-hexane, chloroform, ethyl acetate, and *n*-butanol to separate phenolics (Son et al., 2014). The ethyl acetate fraction which is considered to have the highest phenolics contents was evaporated to dryness and used for the present study (Kumaran & Karunakaran, 2006).

### 2.2. Chemicals

Anti-neurofilament (NF)-L, anti-glyceraldehyde 3-phosphate dehydrogenase (GAPDH), anti-sirtuin 1 (SIRT1), and anti-thymocyte differentiation antigen 1 (Thy-1) antibodies were purchased from Cell Signaling Technology (Danvers, MA, USA). Anti-β-actin antibodies and secondary antibodies were purchased from Santa Cruz Biotechnology (Santa Cruz, CA, USA). 2′,7′-Dichlorofluorescin diacetate (DCFH-DA), 3-(4,5-dimethylthiazol-2-yl)-2,5-diphenyl tetrazolium bromide, dimethyl sulfoxide (DMSO), hydrogen peroxide, iron(II) perchlorate hexahydrate, potassium dioxide, and amyloid β protein ($A\beta_{25-35}$, A4559) were purchased from Sigma-Aldrich Chemical Co. (St. Louis, MO, USA).

### 2.3. Quality control of IGE using HPLC-DAD-ESI-MS analysis

IGE was diluted and filtered through 0.45 μm filter before injection into the HPLC. Constituents of IGE were identified and quantified using Agilent 1100 LC/MSD SL Quadrupole mass spectrometer (Agilent LC/MSD API-Electrospray SL G2708DA) equipped with Shimadzu Prominence (Modular HPLC) system. The HPLC-DAD analysis was performed using Shimadzu which system consisted of DGU-20A on-line degassing unit, LC-20AB solvent delivery unit, SIL-20A autosampler, CMB-20A system controller and SPD M20A photo-diode array detector (DAD). Sunfire™ $C_{18}$ column (5.0 μm, 4.6 mm × 25.0 mm, Waters, Ireland) was used. The gradient solvent of binary mobile phase consisted of 1% formic acid in double deionized water (Solvent A) and 0.1% formic acid in acetonitrile (Solvent B). The gradient was 0 min, 5% solvent B; 0–5 min, 5–15% solvent B; 5–20 min, 15% solvent B; 20–25 min, 15–20% solvent B; 25–30 min, 20% solvent B; 30–35 min, 20–23% solvent B; 35–40 min, 23–25% solvent B; 40–45 min, 25–50% solvent B; 45–50 min, 50–5% solvent B; and 50–60 min, 5% solvent B; with flow rate 1.0 mL/min. Phenolic acid was detected at 280 nm, flavonoid and ellagic acid detected at 360. The condition for HPLC-DAD-ESI-MS consisted of drying gas flow rate was set to 13.0 L/min at 350 °C and nebulizer pressure was 50 psi. The voltage in the positive ion mode was set at 4000 V, 3500 V in negative ion mode and fragmentor voltage was set at 150 V. The mass spectrum was obtained by scanning ions in the range of $m/z$ 100 and 1000. Constituents were characterized by their UV spectra (200–500 nm), retention times relative to external standards, peak spiking, mass spectra and MS fragmentation patterns.

### 2.4. Animals

ICR mice (male, 4 weeks old) were obtained from Samtako Co. (Osan, Korea) and housed 2 per cage in a room maintained with a 12-h light-dark cycle, 55% humidity, and a temperature of 23–25 °C. All animals and experimental procedures were approved by the guidelines established by the Institutional Animal Care and Use Committee (IACUC) of Gyeongsang National University (certificate: GNU-120409-M0009) and in accordance with the Ethical Committee of Ministry of Health and Welfare of Korea.

IGE was dissolved in water and administered orally at a dose of 5, 10, or 20 mg/kg once per day for 3 weeks. The mice were divided into 5 groups: (I) normal control, (II) Aβ (negative control), (III) Aβ + 5 mg/kg IGE, (IV) Aβ + 10 mg/kg IGE and (V) Aβ + 20 mg/kg IGE (n = 8 in each group). The mice were fed with a diet of animal chow and water *ad libitum*. $A\beta_{25-35}$ was administered by intracerebroventricular (ICV) injection to induce memory impairment. Aβ

was dissolved in 0.85% (v/v) sodium chloride solution and each mouse was injected with a Hamilton microsyringe (depth, 2.5 mm; injection volume, 5 μL; dose, 410 pmol per mouse) (Jung Choi et al., 2009).

### 2.5. Culture of RGC-5 cells

The transformed retinal ganglion cell line (RGC-5) was derived by transforming postnatal day 1 rat retinal cells with the $\Psi_2$ EA1 virus (Van Bergen et al., 2009). The RGC-5 line is used widely in glaucoma research because it has certain characteristics of retinal ganglion cells (RGCs), including expression of Thy-1 and brain derived neurotrophic factor (BDNF) (Jang et al., 2013). RGC-5 cells were grown in normal growth medium (Dulbecco's modified Eagle medium (DMEM) containing 5 mM glucose and supplemented with 10% heat-inactivated fetal bovine serum and 100 U/mL penicillin/streptomycin) in a humidified incubator with 5% $CO_2$ at 37 °C. Cultured RGC-5 cells in 96-well plates were used 24 h later for determination of cell viability and microscopic analysis.

### 2.6. Cell viability

Cell viability was measured with the 3-(4,5-dimethylthiazol-2-yl)-2,5-diphenyl tetrazolium bromide (MTT) assay (Jung, Kim, Lee, & Osborne, 2010). In the experiments, $1 \times 10^4$ cells were plated in each well of 96-well plates and allowed to attach to the substrate for a 24 h period. The cells were exposed to lead for an additional 24 h in the absence or presence of different concentrations of IGE. The medium was removed and MTT solution (0.5 mg/mL) was added for 1 h at 37 °C. DMSO solution was added to each well and the plate was shaken for 10 min. The number of living RGC-5 cells in each well was determined by measuring the optical density (570 nm test wavelength and 690 nm reference wavelength) using a spectrophotometer (BioTek Instruments, Winooski, VT, USA), and the percentage viability was calculated.

### 2.7. Measurement of intracellular radical scavenging activity of IGE

Intracellular radical activation within RGC-5 cells was determined using DCFH-DA (Kim, Kang, Lee, Nho, & Jung, 2011). The cells were treated with different concentrations of IGE for 1 h and then treated with DCFH-DA (final concentration, 10 μM) for 15 min at 37 °C. After 15 min, the 96-well plates were washed twice with PBS and then the medium was replaced with fresh medium containing the same compounds without DCFH-DA. The 96-well plates were loaded into a plate-holder fluorescence spectrophotometer and monitored at a 485 nm excitation wavelength and a 535 nm emission wavelength. After each well had been monitored for 30 s as a baseline measurement, the reaction was initiated by adding 1 mM hydrogen peroxide, 1 mM hydrogen peroxide plus 100 μM of iron (II) perchlorate hexahydrate, or 1 mM potassium dioxide, and fluorescence was monitored for 20 min at 37 °C.

### 2.8. Histological analysis of the mouse retina

Enucleated eyes were fixed with 10% formalin for 24 h and embedded in paraffin. The samples were sectioned equatorially at a thickness of 4 μm using an HM340E microtome (Thermo Fisher Scientific, Walldorf, Germany).

Each retinal section was exposed to hematoxylin solution (0.1% hematoxylin, 10% ammonium) for 8 min. The sections were washed 3 times with distilled water and exposed to bluing reagent (0.2% lithium carbonate solution) for 1 min. The sections were rinsed in 95% alcohol, exposed to 1% Eosin Y solution for 1 min, and then washed 3 times with 95% alcohol. The sections were cover slipped with a mounting medium and observed under a light microscope (Olympus, Tokyo, Japan).

Light-microscope images were taken, and the thickness of the inner nuclear layer (INL) was measured by a single observer at several points in the photographs. Observations were restricted to the orientated central zone, and the fovea and peripheral region were avoided. Data from 3 sections were averaged for each eye and used to evaluate the thickness of the INL.

### 2.9. Protein extraction and western blot analysis of the mice retina

The retina was separated from the eye, lysed in RIPA buffer (150 mM NaCl, 1.0% IGEPAL CA-630, 0.5% sodium deoxycholate, 0.1% SDS, 50 mM Tris, pH 8.0, 1× protease inhibitors), and incubated for 30 min at 4 °C. After the incubation, the retina was sonicated and centrifuged at 14,000*g* for 30 min at 4 °C. The supernatant was transferred to a new vessel and the protein concentration was determined using a Bio-Rad Protein Assay kit (Bio-Rad Laboratories, Hercules, CA, USA).

Western blot analysis was performed with anti-NF-L, anti-GAPDH, anti-SIRT1, and anti-Thy-1 primary antibodies (1:3000 dilution; Cell Signaling Technology, Beverly, MA, USA). Secondary antibodies were purchased from Santa Cruz Biotechnology Co. Ltd (1:3000 dilution; Santa Cruz Biotechnology, CA, USA). Immuno-reactive bands were detected using enhanced chemiluminescence reagents (Amersham Bioscience, GE Healthcare, UK) and measured via densitometry using an LAS-4000 image reader and Multi Gauge 3.1 software (Fuji Photo Film, Japan).

### 2.10. Statistical analysis

The data in this study are presented as the mean ± standard error of the mean (SEM). Statistical comparisons were made using one-way ANOVA followed by Dunnett's test. Statistical analyses were conducted using SigmaPlot (Systat Software, Inc., San Jose, CA, USA) and significance was determined using the p-value of the results ($^{*}$ $p < 0.05$, $^{**}$ $p < 0.01$, $^{***}$ $p < 0.001$).

## 3. Results

### 3.1. Effect of IGE on cell viability

IGE was used at concentrations of 1–100 μg/mL in the *in vitro* experiments, and IGE at these concentrations had no effect on the viability of RGC-5 cells (Fig. 1).

### 3.2. Effect of IGE on intracellular ROS level

Following oxidative insult by $H_2O_2$, $O_2$, or OH, intracellular ROS levels were increased by 383.35%, 162.12%, and 615.03%, respectively, relative to the control cells (Fig. 2). However, IGE treatment at 1, 5, 10, 50, and 100 μg/mL significantly inhibited radical activity in RGC-5 cells and decreased intracellular radical formation in a dose-dependent manner.

### 3.3. Histological findings from Aβ-induced retinal damage in vivo

The results from the histological hematoxylin and eosin staining assay are shown in Fig. 3. Aβ administration changed the cell density of the ganglion cell layer and the thickness of the inner plexiform layer, or outer nuclear layer. However, relative to normal tissue (Fig. 3A, a), samples from mice that were injected Aβ exhibited a significant thinning of the inner nuclear layer (INL) and outer nuclear layer (ONL) (Fig. 3A, b), which appeared to have been inhibited in tissues treated with IGE (Fig. 3A, c, d, and e).

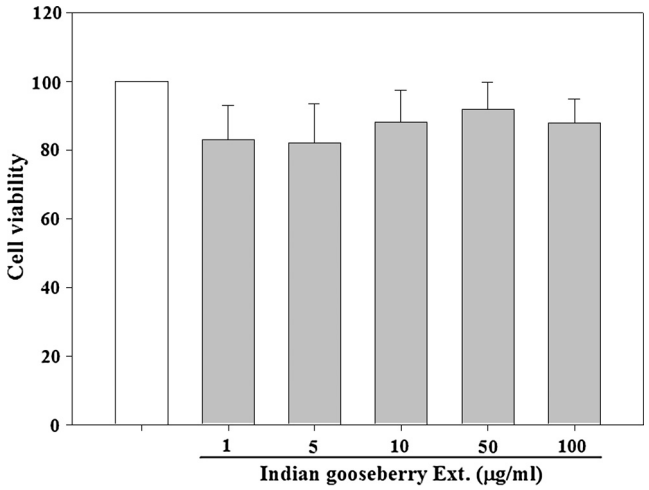


**Fig. 1.** The effect of Indian gooseberry on the viability of RGC-5 cells. The cells were treated with the indicated concentrations of Indian gooseberry extracts (IGE) for 24 h, and cell viability was determined by the MTT assay as described in Section 2. Data are presented as the mean ± SEM of 3 independent experiments.

The average thickness of the INL + ONL in Aβ-injected mice was reduced in comparison with that of the control group at several points of measurement (200 μm superior: 25.59 ± 1.46 versus 40.30 ± 2.51 μm, $p < 0.001$; 200 μm inferior: 23.97 ± 0.24 versus 42.71 ± 5.69 μm, $p < 0.001$; 600 μm superior: 25.79 ± 2.60 versus 40.57 ± 1.01 μm, $p < 0.01$; 600 μm inferior: 26.28 ± 2.41 versus 37.81 ± 3.11 μm, $p < 0.01$). However, the average thickness of the INL + ONL of the mice that were orally treated with 20 mg/kg IGE were significantly protected from the effect of the Aβ administration (200 μm superior: 44.95 ± 3.01 versus 25.59 ± 1.46 μm, $p < 0.001$; 200 μm inferior: 42.37 ± 2.19 versus 23.97 ± 0.24 μm, $p < 0.001$; 600 μm superior: 41.83 ± 0.58 versus 25.79 ± 2.60 μm, $p < 0.001$; 600 μm inferior: 44.10 ± 0.82 versus 26.28 ± 2.41 μm, $p < 0.001$) (Fig. 3B). Oral treatment with 5 and 10 mg/kg IGE also protected against the Aβ-induced reduction in INL + ONL thickness (200 μm superior: 20.03% and 44.21%, respectively; 200 μm inferior: 30.25% and 43.93%, respectively; 600 μm superior: 33.82% and 33.06%, respectively; 600 μm inferior: 10.61% and 32.18%, respectively) in comparison with the negative control treatment (Fig. 3B).

### 3.4. Effects of IGE on Aβ-induced retinal damage in mice

Measurement of Thy-1 and NF-L levels is a reliable method of assessing RGC injury (Chidlow & Osborne, 2003). ICV administration of 410 pmol Aβ decreased expression of Thy-1 and NF-L proteins in the mouse retina. Three days after the Aβ injection, Thy-1 expression in the retina was significantly decreased to 69.78% of that of the normal control group. However, as shown in Fig. 4, oral administration of 5, 10, and 20 mg/kg IGE significantly recovered Thy-1 expression to 90.08%, 119.47%, and 114.22%, respectively, of that of the normal control group (see Fig. 4).

Three days after the Aβ injection, NF-L expression in the retina was significantly decreased to 72.26% of that of the normal control group. However, oral administration of 5, 10, and 20 mg/kg IGE significantly recovered expression of NF-L to 103.03%, 109.50%, and 133.42%, respectively, of that of the normal control group.

To further clarify our findings and explore the effect of Indian gooseberry extract on the retina under Aβ-induced stress, SIRT1 expression levels were evaluated. Aβ administration decreased SIRT1 expression to 81.11% of that of the normal control retinas. However, 20 mg/kg IGE significantly recovered expression of SIRT1 to 124.94% of that of the normal control group ($p < 0.05$) (Fig. 5).

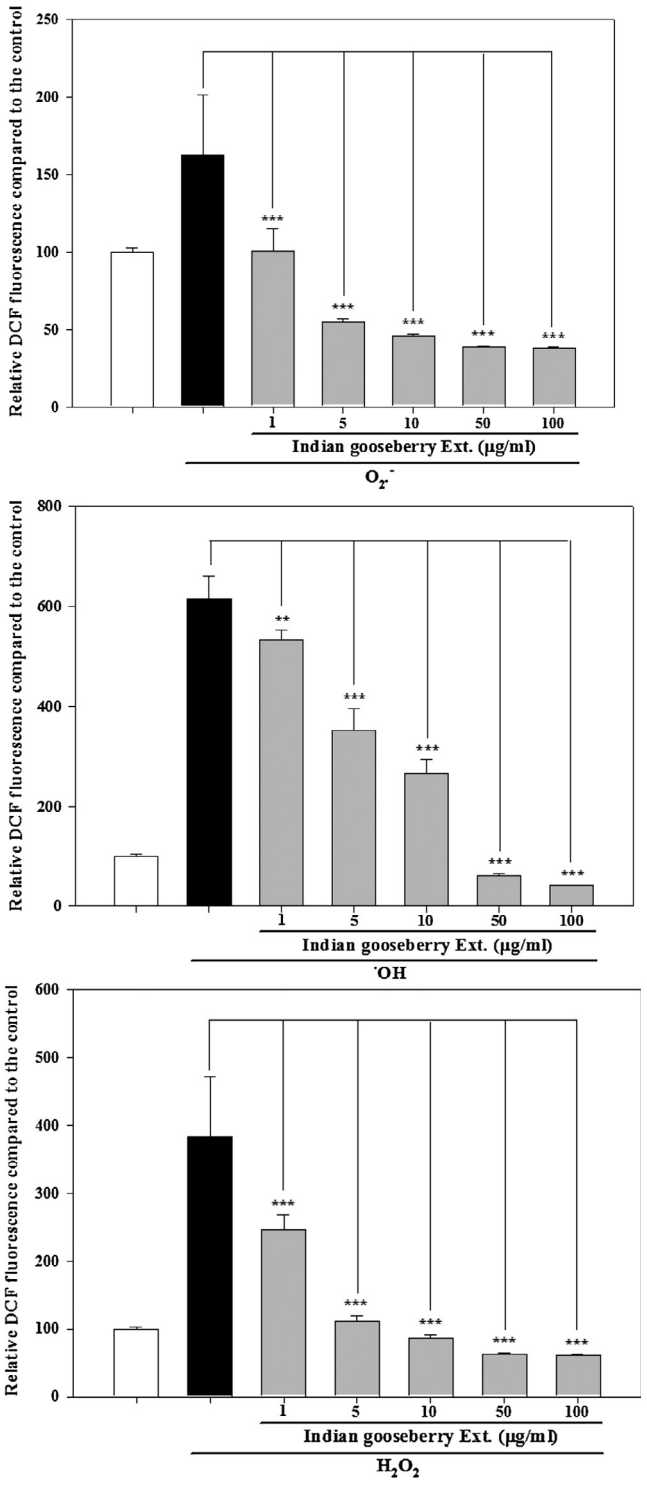


**Fig. 2.** The effects of Indian gooseberry on ROS production induced by $H_2O_2$, $O_2$, and OH. Intracellular ROS levels were determined by measuring the fluorescence of DCFH-DA (485 nm excitation wavelength and 535 nm emission wavelength). Data are presented as the mean ± SEM of 3 independent experiments. Double asterisks (**) indicate $p < 0.01$; triple asterisks (***) indicate $p < 0.001$.

### 3.5. Identification of the compounds from IGE using HPLC-DAD-ESI-MS

The Chromatograms of Indian gooseberry were present in Fig. 6, peaks were determined and the results were indicated in Table 1.

As shown in Table 1 and Fig. 6, the main phenolic compounds that found in IGE were hydrolysable tannins and their glycoside

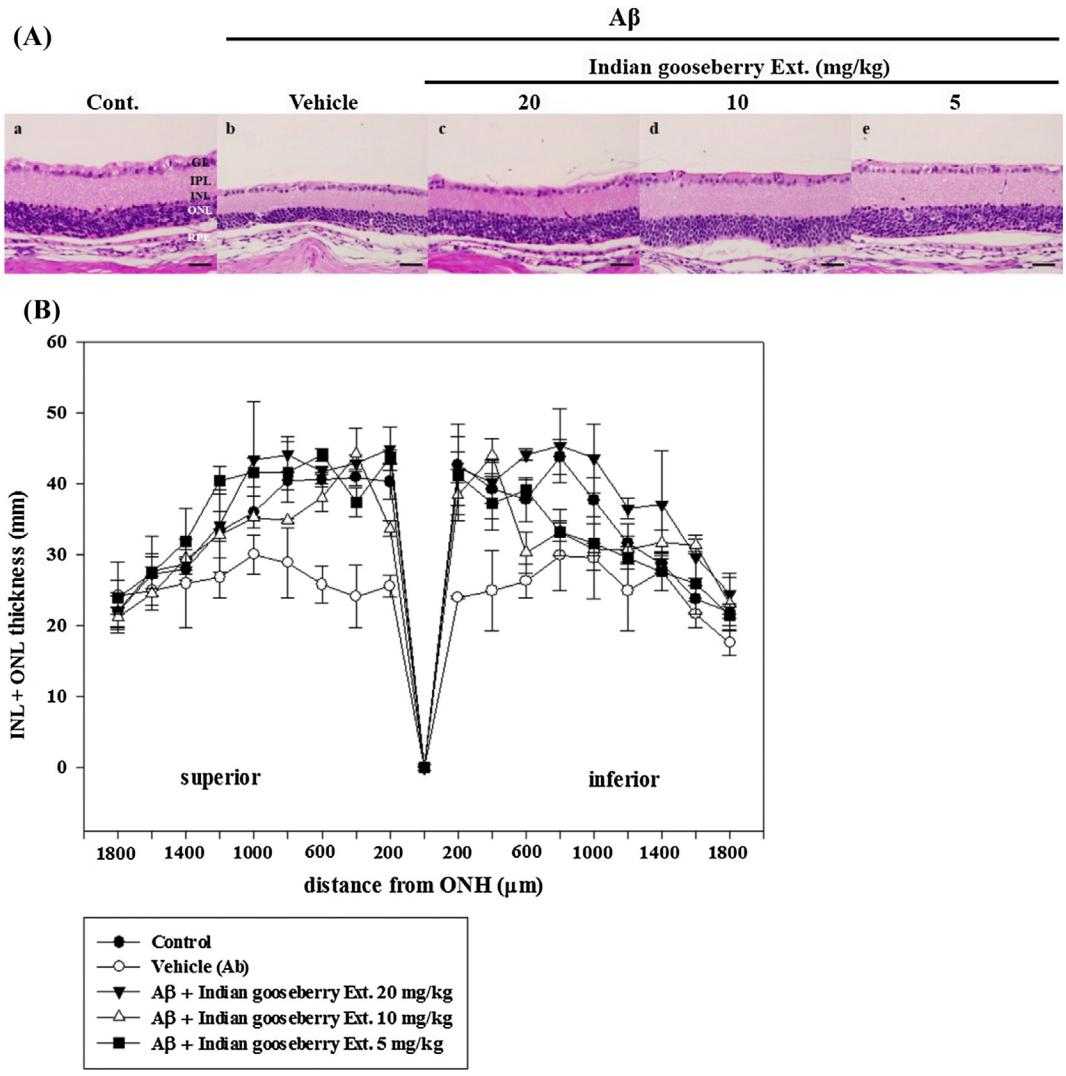


**Fig. 3.** Aβ damage in ICR mice. Hematoxylin and eosin (H&E) staining showed obvious disintegration of the nuclear layers of the retina after Aβ administration. The thicknesses of the inner nuclear layers (INL) and the outer nuclear layers (ONL) from selected groups were measured. (A) H&E staining of retinal sections; control (a), vehicle (b), Aβ + 20 mg/kg IGE (c), Aβ + 10 mg/kg IGE (d), and Aβ + 5 mg/kg IGE (e). (B) Quantification of INL + ONL thicknesses in mice. Data are presented as mean ± SEM (n = 3 for each group). Oral treatment with IGE at 5, 10, and 20 mg/kg significantly protected the inner nuclear layer from Aβ damage. Scale bar = 50 μm.

derivatives. The results were supported by the research of Yang et al. which were previously reported hydrolysable tannins in Indian gooseberry (Yang, Kortesniemi, Liu, Karonen, & Salminen, 2012).

## 4. Discussion

Our results show that ICV administration of Aβ causes retinal damage, and IGE protects the retina against Aβ-induced toxicity. This is the first demonstration of the capacity of ICV Aβ to induce retinal degeneration *in vivo*, as well as the first demonstration of the protective effect of a berry against retinal degeneration induced by Aβ toxicity. Moreover, our results show that IGE inhibits retinal degeneration caused by Aβ peptides by scavenging free radicals and increasing protein abundance of genes such as SIRT1.

Aβ peptides are cleaved from amyloid precursor protein by β- and γ-secretases. The monomer of Aβ is not toxic; however, Aβ peptide aggregation damages neurons (Kadowaki et al., 2005). Moreover, Aβ is a major component of AD plaques and is also present in drusen in patients with age-related macular degeneration (Guo et al., 2010a). Laboratory studies have shown that oxidative stress, including protein oxidation, lipid peroxidation, and ROS generation, is a possible mechanism underlying Aβ-mediated neurotoxicity (Yatin, Varadarajan, & Butterfield, 2000), and this finding is supported by the evidence that Aβ-induced neuronal damage is inhibited by antioxidants such as vitamin E, folate, acetyl-l-carnitine, and *Ginkgo biloba* constituents (Dhitavat, Ortiz, Rogers, Rivera, & Shea, 2005; Yao, Drieu, & Papadopoulos, 2001).

Indian gooseberry has antioxidant activity and neuroprotective effects. The anti-oxidative effects of Indian gooseberry might be due to the presence of antioxidant phenolic compounds and tannins (Mayachiew & Devahastin, 2008a). In our study, the tested concentrations of IGE did not show toxicity in RGC-5 cells, showing that it was suitable for our study (Jang et al., 2013; Jo, Choi, & Jung, 2013). DCFH-DA was used as a radical probe to quantify intracellular ROS. DCFH-DA penetrates cell membranes and is hydrolyzed by intracellular esterase to form non-fluorescent DCFH (LeBel, Ischiropoulos, & Bondy, 1992). In the presence of ROS such as $H_2O_2$, $O_2$, or OH, DCFH is rapidly oxidized to form highly fluorescent DCF within the cell. The physiological oxidants $H_2O_2$, $O_2$, and OH significantly increased intracellular ROS levels, but ROS

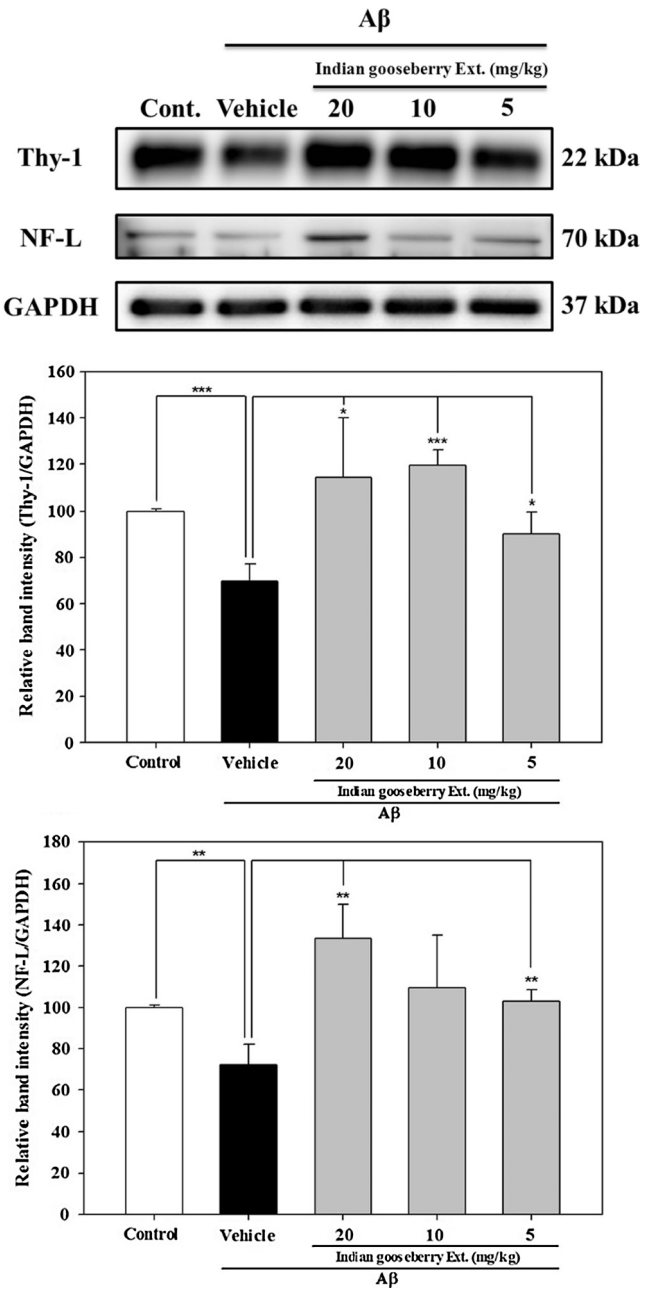


**Fig. 4.** Results of western blot analysis investigating Thy-1 and NF-L expression in the retina 3 days after intracerebroventricular Aβ injection. RGCs were collected from an untreated control mouse, a mouse that underwent Aβ injection only, and mice that underwent Aβ injection and treatment with 5, 10, or 20 mg/kg of IGE. Single asterisks (*) indicate $p < 0.05$; double asterisks (**) indicate $p < 0.01$; triple asterisks (***) indicate $p < 0.001$.

levels were significantly reduced after 1 h of incubation with IGE. Our results indicate that antioxidant constituents of Indian gooseberry are able to permeate through the cell membrane.

Histologic retinal studies in AD patients with optical coherence tomography show retinal nuclear filament layer thinning (Kirbas, Turkyilmaz, Anlar, Tufekci, & Durmus, 2013). Retinal nuclear filament layer thinning in AD is caused by apoptosis of RGCs and atrophy of photoreceptors, which are induced by Aβ, as demonstrated by *in vivo* studies using APP transgenic mice (Tg 2576), APP/PS-1 double transgenic mice, and APPswe/PS1ΔE9 transgenic mice (Guo, Duggan, & Cordeiro, 2010b). In our study, IGE significantly increased INL + ONL thickness in Aβ-treated mice in comparison

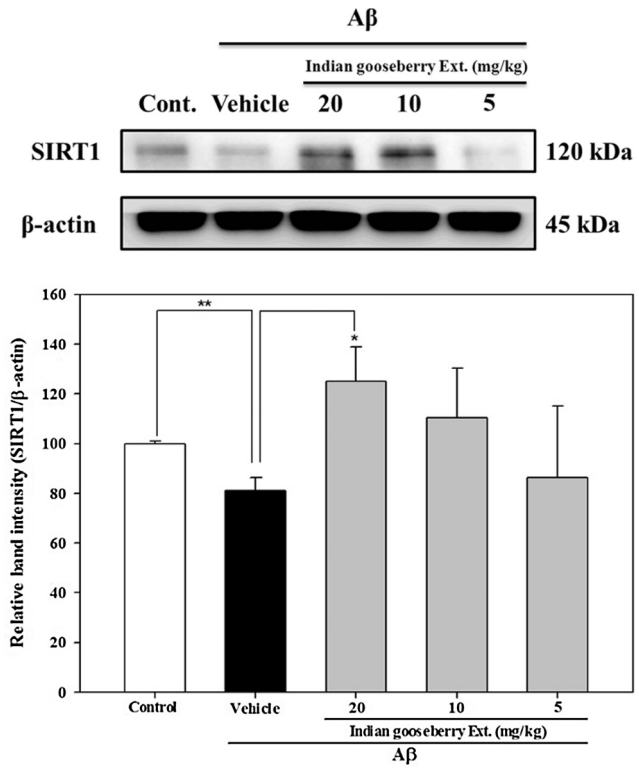


**Fig. 5.** Results of western blot analysis investigating SIRT1 expression in the retina 3 days after intracerebroventricular Aβ injection. Single asterisks (*) indicate $p < 0.05$; double asterisks (**) indicate $p < 0.01$.

with vehicle. The thickness of the INL + ONL is linearly associated with the sensitivity of rod and cone cells (Birch, Wen, Locke, & Hood, 2011). Therefore, increased INL + ONL thickness produced by Indian gooseberry might protect against visual impairment caused by Aβ-induced neurodegeneration.

To determine the protective effect of IGE on the retina, western blot analysis was performed to evaluate the expression of retina-related proteins. Thy-1 is a cell surface glycoprotein that is expressed during RGC differentiation (Lindsey et al., 2013). NF-L is expressed by RGCs in the optic nerve and is therefore used as a measure of RGC viability (Zhang, Safa, Rusciano, & Osborne, 2007). ICV injection of Aβ decreased Thy-1 and NF-L protein abundance; however, oral IGE treatment recovered Thy-1 and NF-L expression to normal levels.

To better understand the intracellular mechanism of action of IGE, SIRT1 protein abundance was measured. SIRT1 is an $NAD^+$-dependent deacetylase that is involved in DNA repair, metabolic regulation, cell stress responses, and cell survival (Donmez & Guarente, 2010; Porcu & Chiarugi, 2005). SIRT1 is activated by the polyphenol resveratrol and has been shown to increase mitochondrial function and promote RGC survival after optic nerve crush (Price et al., 2012; Zuo et al., 2013). A tentative role of SIRT1 in Aβ-induced retinal degeneration could be associated with inflammatory regulation. In fact, Aβ-induced retinal inflammation appears to be regulated by SIRT1 via inhibition of NF-κB (Cao, Liu, Wang, & Wang, 2013). In this study, oral administration of 20 mg/kg IGE significantly up-regulated SIRT1 expression in comparison with that of the control group. This result suggests that Indian gooseberry contains SIRT1 activating compounds that may play a significant role in its protective effect against Aβ-induced retinal degeneration.

Phenolic compounds include hydrolysable tannins and their glycoside derivatives are found in Indian gooseberry. Gallic acid,

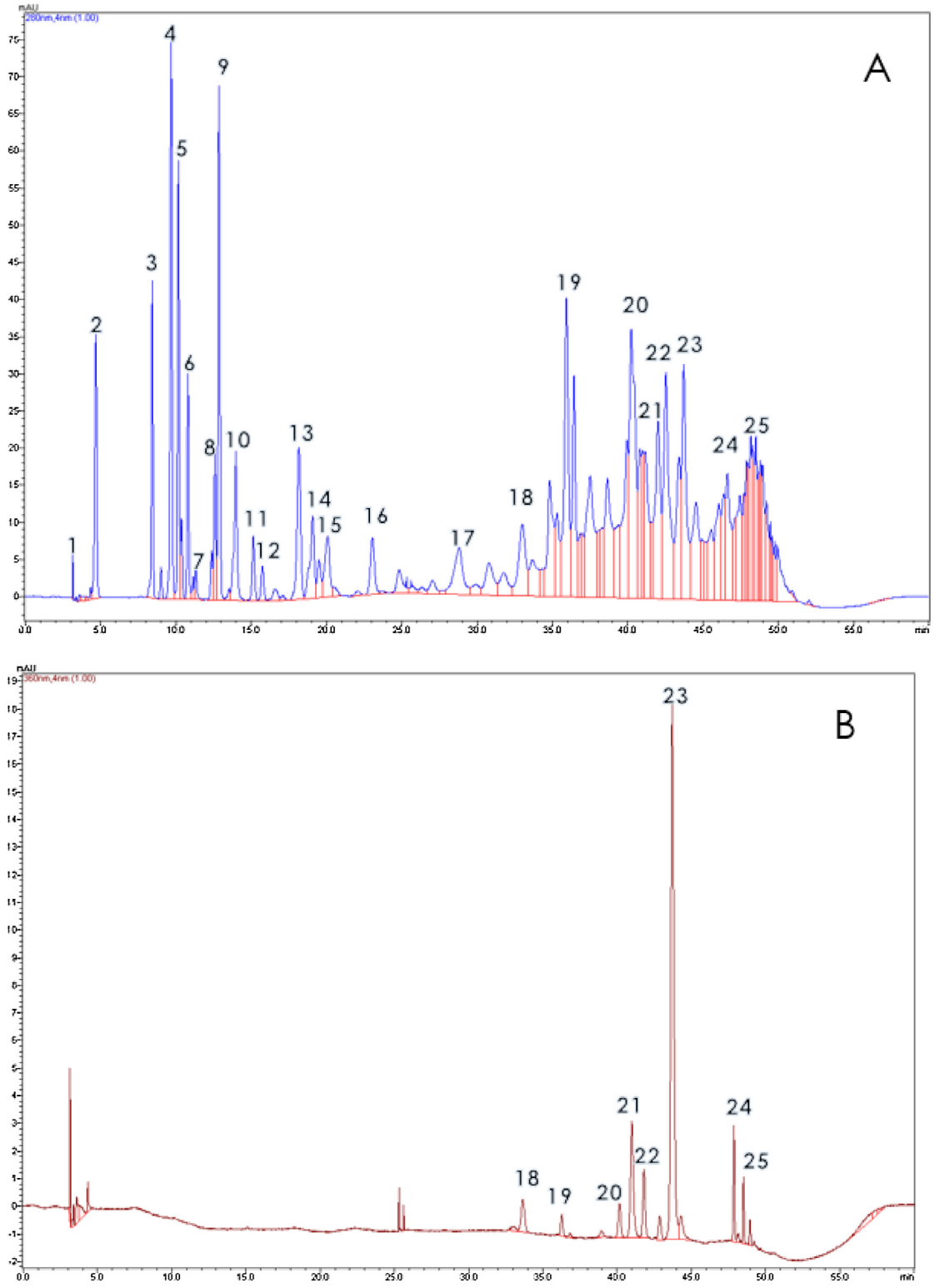


**Fig. 6.** HPLC chromatograms of IGE. The chromatogram was detected at 280 nm (A) and 360 nm (B).

ellagic acid, and their derivatives are common phenolic compounds that found in it (Table 1 and Fig. 6). It has been reported that gallic acid and ellagic acid from *Terminalia chebula* inhibited acetylcholine esterase, and suggested that tannins could be active compounds of *T. chebula* on neurodegeneration (Afshari, Sadeghnia, & Mollazadeh, 2016). Ellagic acid enhanced the activity of intracellular antioxidant enzymes, and improves survival of $Cd^{2+}$-primed astrocyte. This information provides that tannin as antioxidant have beneficial effects on neuronal degeneration, and this might be due to antioxidative effects (C. S. Yang et al., 2008).

In this study, we found that IGE protects the retina against Aβ-induced toxicity in mice, and major constituents of this extract, hydrolysable tannins and their glycoside derivatives, could possibly be the acting compounds due to their antioxidative potency. Therefore, Indian gooseberry consumption may provide health benefits by preventing retinal degeneration.

**Table 1**
Characterization of the compounds in IGE using HPLC-DAD-MS detection.

| Peak | $R_t$ (min) | $\lambda_{max}$ (nm) | MW | MS (*m*/*z*) | Tentative identification |
|---|---|---|---|---|---|
| 1 | 3.12 | 223, 276 | 362 | 361; $[M-H]^-$<br>363; $[M+H]^+$ | Mucic acid gallate |
| 2 | 4.76 | 225, 279 | 362 | 361; $[M-H]^-$<br>363; $[M+H]^+$ | Mucic acid gallate |
| 3 | 8.56 | 225, 278 | 332 | 331; $[M-H]^-$<br>333; $[M+H]^+$ | Galloyglucose (glucogallin) |
| 4 | 9.64 | 225, 278 | 344 | 343; $[M-H]^-$<br>345; $[M+H]^+$ | Mucic acid lactione gallate |
| 5 | 10.02 | 225, 271 | 170 | 433; $[M-H]^-$<br>435; $[M+H]^+$ | Gallic acid |
| 6 | 10.49 | 225, 278 | 344 | 343; $[M-H]^-$<br>345; $[M+H^+$ | Mucic acid lactione gallate |
| 7 | 11.94 | 225, 273 | 514 | 513; $[M-H]^-$ | Mucic acid digallate |
| 8 | 12.28 | 225, 279 | 344 | 343; $[M-H]^-$<br>345 $[M+H]^+$ | Mucic acid lactione gallate |
| 9 | 12.79 | 225, 275 | 484 | 483; $[M-H]^-$<br>485; $[M+H]^+$ | Digalloyl glucose |
| 10 | 13.87 | 225, 276 | 286 | 285; $[M-H]^-$<br>287; $[M+H]^+$ | Malic acid gallate |
| 11 | 14.11 | 225, 269 | 484 | 483; $[M-H]^-$<br>484; $[M+H]^+$ | Digalloyl glucose |
| 12 | 15.50 | 225, 276 | 484 | 483; $[M-H]^-$<br>484; $[M+H]^+$ | Digalloyl glucose |
| 13 | 17.09 | 225, 273 | 496 | 495; $[M-H]^-$<br>497; $[M+H]^+$ | Mucic acid digallate |
| 14 | 18.01 | 225, 275 | 636 | 635; $[M-H]^-$ | Trigalloylglucose |
| 15 | 20.79 | 225, 275 | 952 | 951; $[M-H]^-$ | Geranin |
| 16 | 22.47 | 225, 275 | 636 | 635; $[M-H]^-$ | Trigalloylglucose |
| 17 | 28.45 | 225, 273 | 636 | 635; $[M-H]^-$ | Trigalloylglucose |
| 18 | 33.31 | 225, 272 | 786 | 785; $[M-H]^-$ | Digalloyl HHDP-glucose |
| 19 | 35.13 | 225, 275 | 954 | 953; $[M-H]^-$ | Chebulalic acid |
| 20 | 40.95 | 257, 362 | 448 | 447; $[M-H]^-$ | Ellagic acid deoxyhexose |
| 21 | 41.81 | 257, 362 | 434 | 433; $[M-H]^-$<br>435; $[M+H]^+$ | Ellagic acid pentose |
| 22 | 42.88 | 257, 362 | 448 | 447; $[M-H]^-$ | Ellagic acid deoxyhexose |
| 23 | 43.72 | 253, 368 | 302 | 301; $[M-H]^-$ | Ellagic acid |
| 24 | 47.87 | 256, 348 | 448 | 447; $[M-H]^-$<br>449; $[M+H]^+$ | Quercetin-*O*-3-rhamnoside |
| 25 | 46.70 | 225, 277 | 356 | 355; $[M-H]^-$ | Chebulic acid |

## Author contributions

HJ, PS, WJP, HJH, DK, ST, SHJ, and CYL designed the research; HJ, HJH, and DK conducted the research; HJ analyzed the data and conducted statistical analysis; HJ, SHJ, and CYL wrote the paper, which revised by DK, SHJ and CYL; HJ, SHJ, and CYL are responsible for the final content.

## Acknowledgements

The RGC-5 cells were a generous gift from Alcon Research, Ltd. This work was financially supported by an intramural grant (2Z04930) from the Korea Institute of Science and Technology (KIST), Republic of Korea.

## Conflict of interest

The authors declare no financial conflict of interest.

## References

Afshari, A. R., Sadeghnia, H. R., & Mollazadeh, H. (2016). A review on potential mechanisms of *Terminalia chebula* in Alzheimer's disease. *Advances in Pharmacological Sciences, 2016*, 8964849.

Barthakur, N. N., & Arnold, N. P. (1991). Chemical analysis of the emblic (*Phyllanthus emblica* L.) and its potential as a food source. *Scientia Horticulturae, 47*, 99–105.

Berisha, F., Feke, G. T., Trempe, C. L., McMeel, J. W., & Schepens, C. L. (2007). Retinal abnormalities in early Alzheimer's disease. *Investigative Ophthalmology & Visual Science, 48*, 2285–2289.

Birch, D. G., Wen, Y., Locke, K., & Hood, D. C. (2011). Rod sensitivity, cone sensitivity, and photoreceptor layer thickness in retinal degenerative diseases. *Investigative Ophthalmology & Visual Science, 52*, 7141–7147.

Cao, L., Liu, C., Wang, F., & Wang, H. (2013). SIRT1 negatively regulates amyloid-beta-induced inflammation via the NF-kappa B pathway. *Brazilian Journal of Medical and Biological Research, 46*, 659–669.

Chang, K.-C., Laffin, B., Ponder, J., Énzsöly, A., Németh, J., LaBarbera, D. V., & Petrash, J. M. (2013). Beta-glucogallin reduces the expression of lipopolysaccharide-induced inflammatory markers by inhibition of aldose reductase in murine macrophages and ocular tissues. *Chemico-Biological Interactions, 202*, 283–287.

Chidlow, G., & Osborne, N. N. (2003). Rat retinal ganglion cell loss caused by kainate, NMDA and ischemia correlates with a reduction in mRNA and protein of Thy-1 and neurofilament light. *Brain Research, 963*, 298–306.

Chiu, K., Chan, T. F., Wu, A., Leung, I. Y. P., So, K. F., & Chang, R. C. C. (2012). Neurodegeneration of the retina in mouse models of Alzheimer's disease: What can we learn from the retina? *Age, 34*, 633–649.

Curcio, C. A., & Drucker, D. N. (1993). Retinal ganglion cells in Alzheimer's disease and aging. *Annals of Neurology, 33*, 248–257.

Dhitavat, S., Ortiz, D., Rogers, E., Rivera, E., & Shea, T. B. (2005). Folate, vitamin E, and acetyl-L-carnitine provide synergistic protection against oxidative stress resulting from exposure of human neuroblastoma cells to amyloid-beta. *Brain Research, 1061*, 114–117.

Donmez, G., & Guarente, L. (2010). Aging and disease: Connections to sirtuins. *Aging Cell, 9*, 285–290.

Dutescu, R. M., Li, Q.-X., Crowston, J., Masters, C., Baird, P., & Culvenor, J. (2009). Amyloid precursor protein processing and retinal pathology in mouse models of Alzheimer's disease. *Graefe's Archive for Clinical and Experimental Ophthalmology, 247*, 1213–1221.

Guo, L., Duggan, J., & Cordeiro, M. (2010a). Alzheimer's disease and retinal neurodegeneration. *Current Alzheimer Research, 7*, 3–14.

Guo, L., Duggan, J., & Cordeiro, M. F. (2010b). Alzheimer's disease and retinal neurodegeneration. *Current Alzheimer Research, 7*, 3–14.

Jain, S., & Khurdiya, D. S. (2004). Vitamin C enrichment of fruit juice based ready-to-serve beverages through blending of Indian gooseberry (*Emblica officinalis* Gaertn.) juice. *Plant Foods for Human Nutrition, 59*, 63–66.

Jang, H., Ahn, H. R., Jo, H., Kim, K.-A., Lee, E. H., Lee, K. W., ... Lee, C. (2013). Chlorogenic acid and coffee prevent hypoxia-induced retinal degeneration. *Journal of Agricultural and Food Chemistry, 62*, 182–191.

Jo, H., Choi, S. J., & Jung, S. H. (2013). Protective effects of a compound isolated from *Alnus japonica* on oxidative stress-induced death in transformed retinal ganglion cells. *Food and Chemical Toxicology, 56*, 425–435.

Jung Choi, S., Kim, M. J., Jin Heo, H., Kim, J. K., Jin Jun, W., Kim, H. K., ... Shin, D. H. (2009). Ameliorative effect of 1,2-benzenedicarboxylic acid dinonyl ester against amyloid beta peptide-induced neurotoxicity. *Amyloid, 16*, 15–24.

Jung, S. H., Kim, B. J., Lee, E. H., & Osborne, N. N. (2010). Isoquercitrin is the most effective antioxidant in the plant *Thuja orientalis* and able to counteract oxidative-induced damage to a transformed cell line (RGC-5 cells). *Neurochemistry International, 57*, 713–721.

Kadowaki, H., Nishitoh, H., Urano, F., Sadamitsu, C., Matsuzawa, A., Takeda, K., ... Nagano, T. (2005). Amyloid β induces neuronal cell death through ROS-mediated ASK1 activation. *Cell Death & Differentiation, 12*, 19–24.

Kalt, W., Hanneken, A., Milbury, P., & Tremblay, F. (2010). Recent research on polyphenolics in vision and eye health. *Journal of Agricultural and Food Chemistry, 58*, 4001–4007.

Kim, K.-A., Kang, K. D., Lee, E. H., Nho, C. W., & Jung, S. H. (2011). Edible wild vegetable, *Gymnaster koraiensis* protects retinal ganglion cells against oxidative stress. *Food and Chemical Toxicology, 49*, 2131–2143.

Kirbas, S., Turkyilmaz, K., Anlar, O., Tufekci, A., & Durmus, M. (2013). Retinal nerve fiber layer thickness in patients with Alzheimer disease. *Journal of Neuro-ophthalmology, 33*, 58–61.

Kumar, K. S., Bhowmik, D., Dutta, A., Yadav, A. P., Paswan, S., Srivastava, S., & Deb, L. (2012). Recent trends in potential traditional Indian herbs *Emblica officinalis* and its medicinal importance. *Journal of Pharmacognosy and Phytochemistry, 1*, 18–28.

Kumaran, A., & Karunakaran, R. J. (2006). Nitric oxide radical scavenging active components from *Phyllanthus emblica* L.. *Plant Foods for Human Nutrition, 61*, 1–5.

LeBel, C. P., Ischiropoulos, H., & Bondy, S. C. (1992). Evaluation of the probe 2′,7′-dichlorofluorescin as an indicator of reactive oxygen species formation and oxidative stress. *Chemical Research in Toxicology, 5*, 227–231.

Lindsey, J. D., Duong-Polk, K. X., Dai, Y., Nguyen, D. H., Leung, C. K., & Weinreb, R. N. (2013). Protection by an oral disubstituted hydroxylamine derivative against loss of retinal ganglion cell differentiation following optic nerve crush. *PLoS ONE, 8*, e65966.

Liu, X., Zhao, M., Wang, J., Yang, B., & Jiang, Y. (2008). Antioxidant activity of methanolic extract of emblica fruit (*Phyllanthus emblica* L.) from six regions in China. *Journal of Food Composition and Analysis, 21*, 219–228.

Lu, Y., Li, Z., Zhang, X., Ming, B., Jia, J., Wang, R., & Ma, D. (2010). Retinal nerve fiber layer structure abnormalities in early Alzheimer's disease: Evidence in optical coherence tomography. *Neuroscience Letters, 480*, 69–72.

Mayachiew, P., & Devahastin, S. (2008a). Antimicrobial and antioxidant activities of Indian gooseberry and galangal extracts. *LWT-Food Science and Technology, 41*, 1153–1159.

Mayachiew, P., & Devahastin, S. (2008b). Antimicrobial and antioxidant activities of Indian gooseberry and galangal extracts. *LWT – Food Science and Technology, 41*, 1153–1159.

Mendez, M. F., Mendez, M., Martin, R., Smyth, K. A., & Whitehouse, P. (1990). Complex visual disturbances in Alzheimer's disease. *Neurology, 40*. 439-439.

Miller, M. G., & Shukitt-Hale, B. (2012). Berry fruit enhances beneficial signaling in the brain. *Journal of Agricultural and Food Chemistry, 60*, 5709–5715.

Poltanov, E. A., Shikov, A. N., Dorman, H. J. D., Pozharitskaya, O. N., Makarov, V. G., Tikhonov, V. P., & Hiltunen, R. (2009). Chemical and antioxidant evaluation of Indian gooseberry (*Emblica officinalis* gaertn., syn. *Phyllanthus emblica* L.) supplements. *Phytotherapy Research, 23*, 1309–1315.

Porcu, M., & Chiarugi, A. (2005). The emerging therapeutic potential of sirtuin-interacting drugs: From cell death to lifespan extension. *Trends in Pharmacological Sciences, 26*, 94–103.

Price, N. L., Gomes, A. P., Ling, A. J. Y., Duarte, F. V., Martin-Montalvo, A., North, B. J., ... Sinclair, D. A. (2012). SIRT1 is required for AMPK activation and the beneficial effects of resveratrol on mitochondrial function. *Cell Metabolism, 15*, 675–690.

Rizzo, M., Anderson, S., Dawson, J., Myers, R., & Ball, K. (2000). Visual attention impairments in Alzheimer's disease. *Neurology, 54*, 1954–1959.

Rizzo, M., Anderson, S. W., Dawson, J., & Nawrot, M. (2000). Vision and cognition in Alzheimer's disease. *Neuropsychologia, 38*, 1157–1169.

Roher, A. E., Lowenson, J. D., Clarke, S., Woods, A. S., Cotter, R. J., Gowing, E., & Ball, M. J. (1993). beta-Amyloid-(1–42) is a major component of cerebrovascular amyloid deposits: Implications for the pathology of Alzheimer disease. *Proceedings of the National Academy of Sciences, 90*, 10836–10840.

Sadun, A. A., & Bassi, C. J. (1990). Optic nerve damage in Alzheimer's disease. *Ophthalmology, 97*, 9–17.

Son, J.-E., Lee, B. H., Nam, T. G., Im, S., Chung, D. K., Lee, J. M., ... Kim, D.-O. (2014). Flavonols from the ripe fruits of *Opuntia ficus*-indica var. *saboten* protect neuronal PC-12 cells against oxidative stress. *Journal of Food Biochemistry, 38*, 518–526.

Srivasuki, K. (2012). Nutritional and health care benefits of Amla. *Journal of Pharmacognosy, 3*.

Van Bergen, N. J., Wood, J. P., Chidlow, G., Trounce, I. A., Casson, R. J., Ju, W.-K., ... Crowston, J. G. (2009). Recharacterization of the RGC-5 retinal ganglion cell line. *Investigative Ophthalmology & Visual Science, 50*, 4267–4272.

Wang, Y., Huo, Y. Z., Zhao, L., Lu, F., Wang, O., Yang, X., ... Zhou, F. (2016). Cyanidin-3-glucoside and its phenolic acid metabolites attenuate visible light-induced retinal degeneration in vivo via activation of Nrf2/HO-1 pathway and NF-B suppression. *Molecular Nutrition & Food Research, 60*, 1564–1577.

Wang, Y., Kim, H. J., & Sparrow, J. R. (2017). Quercetin and cyanidin-3-glucoside protect against photooxidation and photodegradation of A2E in retinal pigment epithelial cells. *Experimental Eye Research, 160*, 45–55.

Wang, Y., Zhang, D., Liu, Y., Wang, D., Liu, J., & Ji, B. (2015). The protective effects of berry-derived anthocyanins against visible light-induced damage in human retinal pigment epithelial cells. *Journal of the Science of Food and Agriculture, 95*, 936–944.

Wang, Y., Zhao, L., Lu, F., Yang, X., Deng, Q., Ji, B., & Huang, F. (2015). Retinoprotective effects of bilberry anthocyanins via antioxidant, anti-inflammatory, and anti-apoptotic mechanisms in a visible light-induced retinal degeneration model in pigmented rabbits. *Molecules, 20*, 22395–22410.

Wyss-Coray, T. (2006). Inflammation in Alzheimer disease: Driving force, bystander or beneficial response? [10.1038/nm1484]. *Nature Medicine, 12*, 1005–1015.

Yang, B., Kortesniemi, M., Liu, P., Karonen, M., & Salminen, J. P. (2012). Analysis of hydrolyzable tannins and other phenolic compounds in emblic leafflower (*Phyllanthus emblica* L.) fruits by high performance liquid chromatography-electrospray ionization mass spectrometry. *Journal of Agriculture and Food Chemistry, 60*, 8672–8683.

Yang, C. S., Tzou, B. C., Liu, Y. P., Tsai, M. J., Shyue, S. K., & Tzeng, S. F. (2008). Inhibition of cadmium-induced oxidative injury in rat primary astrocytes by the addition of antioxidants and the reduction of intracellular calcium. *Journal of Cellular Biochemistry, 103*, 825–834.

Yao, Z.-X., Drieu, K., & Papadopoulos, V. (2001). The Ginkgo biloba extract EGb 761 rescues the PC12 neuronal cells from β-amyloid-induced cell death by inhibiting the formation of β-amyloid-derived diffusible neurotoxic ligands. *Brain Research, 889*, 181–190.

Yatin, S. M., Varadarajan, S., & Butterfield, D. A. (2000). Vitamin E prevents Alzheimer's amyloid ß-Peptide (1–42)-induced neuronal protein oxidation and reactive oxygen species production. *Journal of Alzheimer's Disease, 2*, 123–131.

Zhang, B., Safa, R., Rusciano, D., & Osborne, N. N. (2007). Epigallocatechin gallate, an active ingredient from green tea, attenuates damaging influences to the retina caused by ischemia/reperfusion. *Brain Research, 1159*, 40–53.

Zuo, L., Khan, R. S., Lee, V., Dine, K., Wu, W., & Shindler, K. S. (2013). SIRT1 promotes RGC survival and delays loss of function following optic nerve crush. *Investigative Ophthalmology & Visual Science, 54*, 5097–5102.